24th INTERNATIONAL CONGRESS ON SOUND AND VIBRATION
23–27 July 2017, London

ICSV24
23-27JULY 2017
LONDON CALLING

INVESTIGATION OF ATTENUATION MECHANISM OF NON-LINEAR DAMPER FOR SUPPRESSION OF MICRO-VIBRATION ON A CAR BODY

Hiroki NAKAMURA, Toru YAMAZAKI

Department of mechanical engineering, Kanagawa University, 3-27-1, Rokkakubasi, Kanagawa-ku, Yokohama, Japan
email: hiroki-nak@kanagawa-u.ac.jp

Toshiaki KAMO, Hideki OHSAWA, Hiroshi SAKANOUE

Yamaha Motor Co., Ltd, Japan

The present damper developed for a micro vibration suppression of a car body, that uses an oil hydraulic pressure control valve for generating damping force, is able to produce a velocity-independent nearly constant damping force unlike an ordinary viscous damper and hence to produce a large damping force even in a very small velocity range. Previous report elucidated firstly the generation mechanism of damping force in quasi-static state and then derived the equation for attenuation characteristics, specifically derived the damping coefficient by linearizing the nonlinearity due to a built-in oil hydraulic pressure control valve by using describing function method.
In this paper, firstly the attenuation model is enhanced in order to be able to estimate damping characteristics of the test damper more precisely even in dynamic state by introducing the time-delay elements into the previous model. Then the validity of modelling of damping mechanism is verified on the basis of comparison of simulations with experiments. Finally, it is concluded clearly that the present modified model can simulate the characteristics of damping force vs piston speed more precisely than original model.

Keywords: Body vibration while driving, Dynamic model, Device technology, Damping for micro-vibration

1. Introduction

Reduction of car-frame vibration is strongly desired for better performance, maneuverability and comfort. However, conventional viscus dampers do not perform well because amplitude of car-frame vibration is very small. Then, the non-linear damper (so called performance damper) is developed for a micro vibration suppression of a car body; that uses an oil hydraulic pressure control valve for generating damping force, is able to produce a velocity-independence nearly constant damping force[(1)].

An example installation of a performance damper is shown in figure 1. As shown in figure, the damper bridges between two longitudinal frames on both sides, and it suppress micro-vibration of car-frame. Also, another performance damper is equipped in front to enhance vehicle performance.

This study aims on development of optimize design process of assembling best performance damper in an arbitrary car for better performance and more comfort.

Fig.1 Performance damper installed on a car

Previous study(2) has reported about generation mechanism of damping force with pressure control valve and kinematic model (non-linear characteristics) is constructed under quasi-static state, and linearized model of damping force under sinusoidal excitation is constructed based on described function method. Validity of proposed model under quasi-static state (low frequency) is shown through theoretical and experimental analysis. However, simulated damping force deviates from experimental data when piston speed is high (or excitation frequency is high). Thus, more precise model of damping force against piston speed considering response delay of each component which is appropriate for dynamic state is required.

In this report, cause of hysteresis observed in experimental damping force characteristics is investigated, and detailed model considering delay components is constructed. Also, validity of constructed model is examined through simulation and experiment.

2. Characteristics of the Test Damper

2.1 Main components of the test damper

Main components and structure of target performance damper and shown in fig. 2.

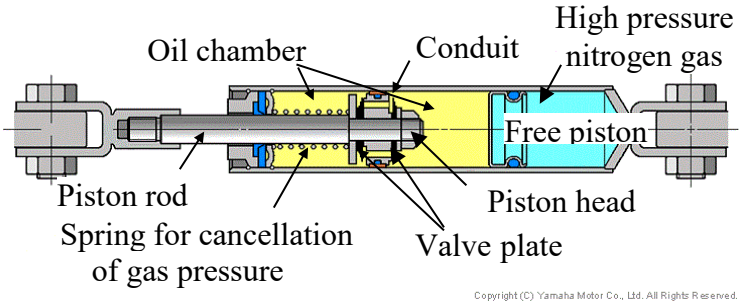

Fig.2 Components of test performance damper

Pressure control valves work as damping elements, which is composed of several conduits and disk valve plates. The level of damping force is designed by changing the disk characteristics: diameter, thickness, and numbers. Also, oil chamber is pressured by high pressure nitrogen gas via free piston, so to prevent drop of bulk modulus. This structure restrains response lag caused by volume effect during very small excitation. Additionally, spring for cancellation of gas pressure enables easy installation on a car.

2.2 Mechanism of damping force generation under quasi-static conditions

As described in previous report [2], Damping force F of under quasi-static condition is consist of constant damping force F_0 stem from cracking pressure and damping force stem from pressure over-

ride, and it is approximated as follows with assumption that leakage at very low speed can be neglected and damping force stem from pressure override is proportional to piston speed (gradient coefficient: α);

$$F = \mathrm{sgn}\left(\frac{\mathrm{d}x}{\mathrm{d}t}\right)F_0 + \alpha\frac{\mathrm{d}x}{\mathrm{d}t} \tag{1}$$

Here, F_0 ($=A_r p_c$) is constant damping force stem from cracking pressure. Equation 1 can be illustrated as fig.3; Damping force rises (or drops) drastically to F_0 (or $-F_0$) around 0 [mm/s], and velocity proportional force with gradient α is added.

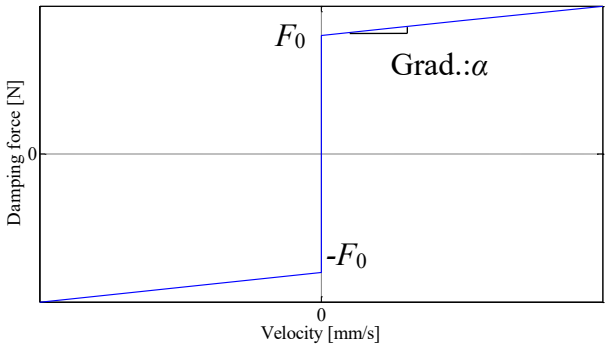

Fig.3 Correlation between velocity and damping force

2.3 Measured damping force under dynamic condition

Sinusoidal excitation test of the target damper is performed with shock absorber tester to observe dynamic characteristics. Apparatus is shown in fig.4. Displacement of piston is measured with an inductive displacement sensor, and damping force is measured with a load cell installed on the edge of cylinder.

Fig.4 Sinusoidal excitation experimental equipment for test damper

Figure 5 is an example data of velocity vs damping force characteristics; excited with 0.5mm amplitude and 40Hz. Here, velocity is calculated by numerical substitution of displacement data. Damping force characteristics due to cracking pressure and pressure override are clearly drawn in the figure.

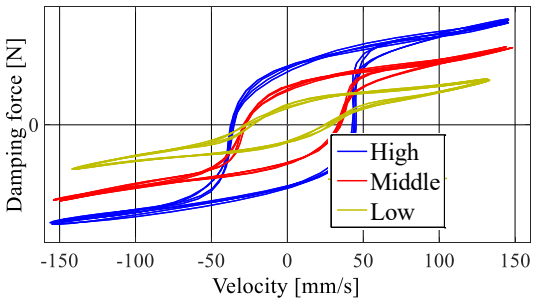

Fig.5 Correlation between velocity and damping force

However, unlikely to the theoretical characteristics shown in fig.3, hysteresis is seen in fig.5 near transition point, where velocity shift its direction. Velocity vs damping force characteristics of dynamic state deviates from quasi-static state. This is mainly because first-order response lag of pressure inside caused by friction of free piston and compressibility of oil (including elasticity of the chamber); while piston is moving, pressure of cylinder P reaches the pressure of gas P_0 with time delay.

In following chapter, mechanism of dominant two factors involving hysteresis is investigated through numerical simulation: pressure fluctuation in the oil chamber and response delay of pressure control valve.

3. Mechanism and modelling of response delay components

3.1 Additional damping force induced by fluctuation in the oil chamber

In previous report [2], Damping force F of under quasi-static condition is derived with assumption that pressure of oil chamber P is always equal to pressure of gas chamber P_0. However, interaction of elasticity of oil in the chamber and resistance of piston slide causes response delay. Then, cause of pressure fluctuation, and additional damping force induced by that pressure fluctuation is theoretically analyzed with fig.6.

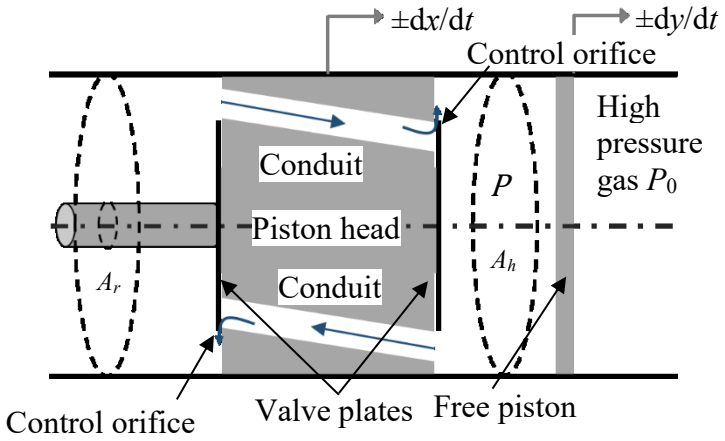

Fig.6 Modelling of pressure control valve for generating constant damping force

Here, top half represents the operation while piston is moving left, and oil flows through conduit from the left. Bottom half represents vice versa.

The free piston drawn on the right slide to balance the pressure of nitrogen gas and the pressure of oil in the right chamber; and control orifice open and close according to the pressure difference of two oil chambers.

Each symbol x, A_h, y, C_v, V, B_d, P, represents piston displacement, pressured area, free piston displacement, damping coefficient related to free piston, volume of oil in a chamber, equivalent volume modulus, and pressure of nitrogen gas respectively. Then, the equation of continuity of oil in the cylinder and the equation of motion of free piston is expressed as follows.

$$A_h \frac{\mathrm{d}x}{\mathrm{d}t} - A_h \frac{\mathrm{d}y}{\mathrm{d}t} = \frac{V}{B_d}\frac{\mathrm{d}P}{\mathrm{d}t} + A_r \frac{\mathrm{d}x}{\mathrm{d}t} \tag{3}$$

$$C_v \frac{\mathrm{d}y}{\mathrm{d}t} = A_h (P - P_0) \tag{4}$$

Following equation is derived from Eqs. 3 and 4 by replacing free piston displacement y.

$$A_p \frac{\mathrm{d}x}{\mathrm{d}t} - \frac{A_h^2}{C_v}(P - P_0) = \frac{V}{B_d}\frac{\mathrm{d}P}{\mathrm{d}t} \tag{5}$$

Here, A_p represents cross section area of the piston rod (A_p=A_h-A_r). Pressure difference of oil and gas is determined Δp, and following equations are derived.

$$A_p \frac{\mathrm{d}x}{\mathrm{d}t} - \frac{A_h^2}{C_v}\Delta p = \frac{V}{B_d}\frac{\mathrm{d}}{\mathrm{d}t}\Delta p \tag{7}$$

Correlation between v and Δp is derived by replacing dx/dt as v (piston speed) and Laplace transforming Eq. 7.

$$A_p v(s) = \left(\frac{V}{B_d}s + \frac{A_h^2}{C_v}\right)\Delta p(s) \tag{8}$$

Eq. 8 can be transposed to clarify relation between input v and output Δp.

$$\Delta p(s) = \frac{A_p}{\frac{V}{B_d}s + \frac{A_h^2}{C_v}} v(s) \tag{9}$$

Here,

$$T = \frac{C_v V}{A_h^2 B_d},\ K = \frac{A_p C_v}{A_h^2} \tag{10), (11}$$

and Eq.9 is transposed as follows

$$\Delta p(s) = \frac{K}{Ts + 1} v(s) \equiv G_1(s) v(s) \tag{12}$$

i.e. pressure fluctuation Δp against piston speed v is first order delay characteristics with time constant T. This pressure fluctuation Δp causes additional damping force $F_1(s)$ expressed as follows.

$$F_1(s) = A_p \Delta p(s) = A_p G_1(s) v(s) \tag{13}$$

Yet the additional damping force caused by pressure fluctuation of oil does not effect when C_v=0, because $G_1(s)$=0.

3.2 Modelling of damping force generated by pressure control valve

In previous report [2], inertia and damping on moving parts (valve plates, specifically) are neglected and restoring force of mechanical spring is only considered to construct damping force model of the performance damper under quasi-static condition based on static characteristics of pressure vs flow rate. In this section, damping force under dynamic state is modelled by considering dynamic characteristics of moving parts of pressure control valve. To simplify the discussion, each control orifice is modelled as fig.7 with assumption that each conduit is covered with a valve plate respectively, even an actual performance damper is composed of several conduits and one valve plates on each side of the piston head.

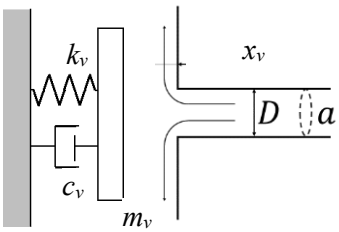

Fig.7 Model of a plate–type pressure control valve

3.2.1 Force equilibrium around the valve plate

Force balance around the valve plate under static/dynamic condition can be described as follows: here, p, x_v, $x_{v.0}$, m_v, c_v, k_v and a represent pressure drop, gap between the valve and the conduit, initial distortion of the valve spring, mass of the valve plate, viscus damping coefficient, stiffness of valve spring, and pressured surface area respectively. $x_{v.s}$ and $x_{v.d}$ represent gap between the valve and the conduit under static and dynamic condition respectively.

Under static condition:
$$ap = k_v(x_{v.s} + x_{v.0}) \tag{14}$$

Under dynamic condition:
$$ap = m_v \frac{d^2 x_{v.d}}{dt^2} + c_v \frac{dx_{v.d}}{dt} + k_v(x_{v.d} + x_{v.0}) \tag{15}$$

3.2.2 Relation between damping force of the target damper and valve gap

The damping force of the target damper under static condition F_s and under dynamic condition F_d can be described as follows with pressured area of piston rod A_r

Under static condition:
$$F_s = A_r p = A_r \frac{k_v}{a}(x_{v.s} + x_{v.0}) \tag{16}$$

Under dynamic condition:
$$F_d = A_r p = A_r \frac{k_v}{a}(x_{v.d} + x_{v.0}) \tag{17}$$

3.2.3 Relation between dynamic damping force F_d and static damping force F_s

In this study, initial value of damping force is approximated 0 (specifically $x_{v.0}$=0) to simplify the simulation. Following equation is derived by Laplace transform of Eqs. 14 to 17 and substitute Eq.14 into Eq.16.

$$F_d(s) = A_r \frac{k_v}{a} \cdot \frac{ap}{ms^2 + c_v s + k_v} \tag{18}$$

And Eq.15 is substituted to Eq.18 as follows

$$F_d(s) = A_r \frac{k_v}{a} \cdot \frac{ak_v x_{v.s}(s)/a}{ms^2 + c_v s + k_v} \tag{19}$$

The, Eq.16 is substituted to Eq.19

$$F_d(s) = \frac{k_v}{ms^2 + c_v s + k_v} F_s(s) \tag{20}$$

So, dynamic damping force F_d and static damping force F_s can be described as follows with transfer function $G_2(s)$.

$$F_d(s) = G_2(s) \cdot F_s(s) \tag{21}$$

In this study, each parameters are schematically estimated based on measured data. Also, following assumption is taken into account even Eq. 21 is practical only when $x_{v.0}$=0; second order delay $G_2(s)$ also effect on F_0, and dynamic damping force F_d is calculated by substituting Eq.1 to static damping force F_s.

Here, pressure fluctuation caused by free piston and motion of pressure control valve are assumed independent, and damping force generated by target performance damper is the sum of pressure difference around piston rod and free piston.

4. Simulations and discussions about delay components

4.1 Simulation Model

Validity of delay components mentioned in previous chapter is examined by comparing experimental data and simulation based on nonlinear characteristics described as Eq. 1 and transfer functions $G_1(s)$ and $G_2(s)$. Simulation model is shown as a block diagram shown in fig.8. As mentioned in previous chapter, sliding of piston induces pressure fluctuation around free piston and pressure control valve, and sum of those pressure difference generates damping force F.

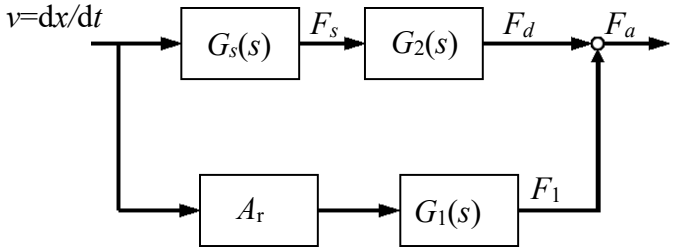

Fig.8 Block diagram of delay system explaining the hysteresis appeared in the measured damping force vs piston speed

4.2 Conditions

Sinusoidal excitation simulation of the target damper is performed; Every 10Hz from 10Hz to 40Hz with amplitude 0.5mm, 4 conditions in total.

4.3 Result

Validity of the proposed model is examined by comparing with experiment. Estimated piston speed vs damping force characteristics is shown in fig.9 (blue line). Also, experimental result is shown in blue line. Compared to the damping force calculated with previous model (shown in fig.8), the new model accurately follows experiment by including response delay of free piston and pressure control valve.

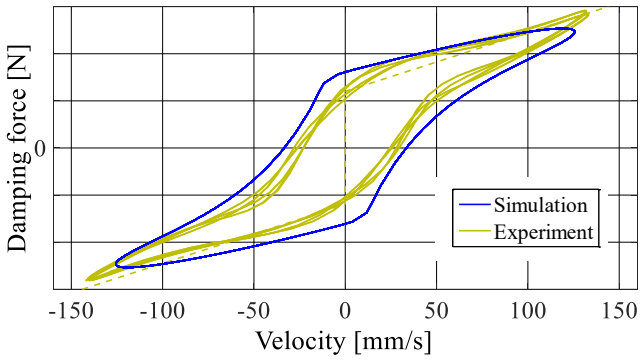

Fig.9 comparison between experiment and simulation at 40Hz

5. Concluding Remarks

In this paper, modelling of the damping mechanism of has reported. The model reported in previous report has improved by integrating detailed delay components model, and its accuracy is validated by comparing experiment and simulation.

Further, the proposed model is expected to be used for optimization of designing damping characteristics of arbitrary vibration systems.

6. Acknowledgement

We deeply appreciate Emeritus Professor of Kanagawa University Eiichi Kojima about giving us constructive comments and warm encouragement

REFERENCES

1 S. Sawai, H. Okada, T. Kamo, Development of Chassis Damping Technology by Hydraulic Damper, Proceedings of 2014 JSAE annual congress(spring), No.120-14 pp19-24, 2014 (In Japanese)

2 H. Nakamura, T. Kamo, H. Ohsawa, S. Fukushima, H. Sakanoue, T. Yamazaki, Modeling of an Attenuation Characteristics of the Damper Used for Micro Vibration of a Car Body, JSAE Transaction, No.47-6, pp.1367-1372, 2016 (In Japanese)